Diphenyl ditelluride assisted synthesis of noble metal-based Silver-Telluride 2D organometallic Nanofibers with enhanced aggregation-induced emission (AIE) using oleylamine.

Carlos Lodeiro (cle@fct.unl.pt)
NOVA School of Science and Technology - NOVA University Lisbon https://orcid.org/0000-0001-5582-5446

Jamila Djafari
Frederico Duarte
Javier Fernández-Lodeiro
Adrián Fernández-Lodeiro
Hugo Santos
Eva Bladt
Sara Bals
Aikaterini Flessa Savvidou
Luis Balicas
Benito Rodriguez-González
Alcindo Dos Santos
José Luis Capelo-Martínez

Article

Keywords:

Posted Date: April 19th, 2023

DOI: https://doi.org/10.21203/rs.3.rs-2808063/v1

Abstract

Silver-Telluride 2D organometallic nanofibers using diphenyl ditelluride (DPDT) as a precursor were synthesized. The synthesis was carried out by reacting DPDT with $AgNO_3$ in acetonitrile at room temperature (RT) under an inert atmosphere. The resulting material was fully characterized using various techniques, including UV-VIS-NIR spectroscopy, steady-state and excited-state fluorescent spectroscopy, IR-FTIR-ATR spectroscopy, HR ESI MS spectrometry, high-resolution transmission electron microscopy (HRTEM), BF-STEM or HAADF-STEM, and confocal fluorescence microscopy images and conductivity measurements. Initially, the nanofibers were almost non-emissive. However, a remarkable modification was observed after treating the nanofibers with oleylamine under ultrasound treatment. This methodology induced an aggregation emission effect (AIE) in the solution and in the solid state, resulting in the formation of a highly red emissive fluorescent nanomaterial. This research provides valuable insights for developing new fluorescent materials with potential applications in various optical fields.

Initially, the nanofibers were almost non-emissive. However, we observed a remarkable modification after treating the nanofibers with oleylamine under ultrasound treatment. This treatment induced an aggregation emissive effect (AIE) in the solution and solid state, resulting in the formation of a highly red emissive fluorescent material.

Overall, our findings demonstrate the successful synthesis of 2D Silver-Telluride 2D organometallic nanofibers and the induction of AIE in the resulting material through oleylamine treatment. This research provides valuable insights for developing new fluorescent materials with potential applications in various fields.

Introduction

Diorganyl ditellurides (RTe – TeR) have emerged as a versatile precursor for synthesizing various metal telluride nanomaterials and nanocrystal ligands, attracting significant attention from the scientific community.[1] The relatively weak Te – Te bonds present in diorganyl ditellurides can be easily cleaved under mild thermolytic or photolytic conditions, making them suitable for manufacturing different metal-telluride or telluride nanocrystals such as CdTe[2], SnTe[3], tellurium nanorods[4], and others, via solvothermal, photolytic, or vapour deposition processes.

Of particular interest are tellurium-containing silver materials, which have potential applications in harvesting thermal and mechanical energy as well as in the production of insulator materials. These materials offer unique optical and electronic properties that make them highly attractive for use in various fields, including electronics, photonics, and renewable energy.[5,6]

Overall, the use of diorganyl ditellurides as a precursor for the synthesis of metal telluride nanomaterials and nanocrystal ligands is a promising area of research, with many potential applications in various

fields. Further research in this area will likely yield valuable insights into the properties and potential applications of these materials.

In the field of coordination chemistry, diorganyl ditelluride (RTe-TeR) species are promising ligands due to their bonding flexibility, redox properties, and multidenticity. They can be used to fabricate metal or metal chalcogenide nanomaterials using relatively softer chemical routes. For example, our group has reported on the ability of diphenyl ditelluride (DPDT) to reduce Au(III) into well-defined spherical gold nanoparticles (AuNPs) in acetonitrile solution at room temperature. This process occurs via Te-Te oxidative cleavage with the concomitant formation of gold nanoparticles and halogenated tellurium derivatives as a subproduct. Controlled oxo-hydrolysis of such halogenated entities and photodecomposition of DPDT generate an oligomeric organotellurium structure deposited over the gold cores, leading to highly stable core@shell nanoparticles.[7]

In addition to gold, platinum(IV) can also be used as a metal precursor in the presence of diorganyl ditelluride derivatives. Partial reduction of Pt(IV) generates highly monodisperse Pt-Te organometallic nanoparticles, which can be used as a single-source precursor to manufacture well-defined $PtTe_2$ multi-crystal nanoparticles under a solvothermal process.[8]

Overall, the use of diorganyl ditellurides in coordination chemistry is a promising area of research that can lead to the development of novel and efficient routes for synthesizing metal and metal chalcogenide nanomaterials. Further research in this field is expected to yield valuable insights into the properties and potential applications of these materials.

Regarding the reaction of Ag(I) with diorganyl ditellurides, several years ago, Wen-Feng Liaw *et al.*[9] reported the formation of organometallic dimers or polymers reacting different diorganyl ditellurides with $AgBF_4$. In the case of DPDT, the authors reported the spontaneous organometallic polymeric formation, revealing the high reactivity of DPDT towards Ag(I), albeit the product partially decomposed under vacuum at ambient temperature, hampering their conditions any further characterization.

Aggregation-induced emission (AIE) is a fascinating photophysical phenomenon that has attracted significant attention in recent years. Unlike traditional luminophores, which often exhibit decreased luminescence upon aggregation, AIE materials become highly emissive when aggregated or in the solid state. This process is intriguing and has revolutionized our understanding of how aggregation affects luminescence.[10]

The development of luminescent materials is crucial for improving human life, and AIE has led to groundbreaking discoveries in this field. AIE fluorogens, also known as AIEgens, possess remarkable photophysical properties that have led to their exploration in various applications, including biosensing and therapeutics, optoelectronic and green energy devices, and environmental monitoring, among others.

One significant advantage of AIE materials is their ability to emit strong fluorescence in the aggregated state, making them useful in designing fluorescent probes for detecting various biological targets,

including proteins, nucleic acids, and small molecules. In addition, AIE materials have been used as imaging agents for cancer diagnosis and therapy, as they can selectively accumulate in tumor tissues and emit bright fluorescence upon aggregation.

AIE materials have also shown promising potential in optoelectronic applications such as organic light-emitting diodes (OLEDs) and organic photovoltaics (OPVs). Their unique properties, such as high quantum yield and efficient energy transfer, make them suitable for these applications.

Moreover, AIE materials have attracted significant interest in the field of green energy, particularly in the design of luminescent solar concentrators (LSCs). These materials can efficiently absorb and convert sunlight into electricity and have potential applications in building-integrated photovoltaics and portable devices. Further research in this area is expected to yield valuable insights and lead to the development of novel AIE materials with enhanced photophysical properties and expanded applications.

Results And Discussion

Following our interest in developing new synthetic routes based on organic ditellurides to prepare noble metal-based nanomaterials, we explore the reactivity of DPDT with $AgNO_3$ in acetonitrile at room temperature under inert atmosphere. Early, Wen-Feng Liaw *et al.*, investigated the interaction of diorganyl ditellurides in a molar relation Ag/Te-Te of 1/2 or 1/3. In our case, the reaction was adjusted to start with a molar ratio Ag(I)/DPDT 1/0.55 using acetonitrile as the solvent under a N_2 atmosphere. In a representative experiment, a freshly prepared solution of DPDT, in acetonitrile was injected into an acetonitrile solution of $AgNO_3$ at room temperature. The solution acquires an initial red colour that, after stirring for 30 min, evolves into forming a red precipitate with a fibrillar aspect. A stable red solution was obtained upon purification in acetonitrile using centrifugation, which did not precipitate even after several days in the solution.

High-resolution transmission electron microscopy (HRTEM) analysis was performed to characterize the material (Fig. 1A). The HRTEM analysis revealed the formation of long nanofibers with thicknesses of 10–20 nm and with intricate nano structure (Fig. 1B). Interestingly, we observed an evident alignment of internal granular electron-dense nanostructures of 1.5-2 nm along the fiber and separated by a channel of about 3.5 nm (**Figure S1A, B**), which are more pronounced in the BF-STEM or HAADF-STEM images shown in Figs. 1C and 1D. Albeit the dark areas, related to the higher atomic number elements (Ag and Te), did not show crystal phases observed in the HRTEM images (**Figure S1C**), the electron diffraction (ED) showed a pattern of rings that can be related to the formation of really small crystallites with planes not yet very well defines, or small crystalline nanoclusters (Fig. 1E).

However, unfortunately, the nanofibers showed limited electron beam stability during microscopy studies. HAADF-STEM investigation at 120 and 300 kV showed that the nanofibers degrade upon electron beam scanning after $t > 10$ sec (see **Figure S2**), which limite our ability to accurately determine their structure. Based on the EDX spectrum, was found ca. 53% of Ag and ca. 47% of Te (see **Figure S3**).

The UV-VIS absorption spectrum of the nanofiber in acetonitrile solution showed two intense absorption peaks centred at ca. 476 nm and 568 nm with comparable relative intensities (Fig. 1F). To further investigate the origin of the observed bands, spectroscopy measurements of the DPDT in acetonitrile were performed. Initially, its solution presents an absorption peak at ca. 397 nm corresponding to the transition nTe – σ* (Te–Te CT band).[7] After reaction with the silver salt, the formation of two absorption bands at low energy was observed (see **Figure S4**). Although the peak at 476 nm could be related to the formation of a metal complex between Ag(I) and DPDT, the peak observed at lower energy (568 nm) is reminiscent of discrete energy levels in quantum confined semiconductor nanocrystals (NCs), albeit a residual fluorescent emission was observed. In our previous work on the reactivity of DPDT with Au(III), we have observed the formation of a four-coordinated organometallic complex $[Au(DPDT)_2]+$ after a partial reduction of Au(III) to Au(I) mediated by the Te-Te moiety, that subsequently evolves towards metallic AuNPs. Since the crystal structures were not evident in electron microscopy images, this absorption at 568 nm should be associated with the transition band rather than a plasmonic origin.

To further investigate the formation of the nanofibers, electrospray ionization mass spectrometry (ESI-MS) was performed during the reaction. As shown in **Figure S5**, after the first minute of reaction, the two more intense signals at 518.791 and 928.684 m/z can be assigned to the formation of the monometallic complexes $[(Ph_2Te_2)Ag]+$ and $[(Ph_2Te_2)_2Ag]+$ respectively (theoretical mass of: 518.791 and 928.681 m/z respectively (see **Figure S6**. With the progress of the reaction (*ca.* 5 min), some structures at a higher m/z ratio indicate the evolution of the monometallic complex. For example, the signal at 1847.2457 m/z can be assigned to the tetra metallic multicentre complexes, such as $[(Ph_2Te_2)_3Ag_4(NO_3)_3]^+$ (theoretical calc. mass of 1847.245 m/z. If we consider the preferential coordination of silver centres (n_c = 2) and based on the complexes observed in the mass spectrometry analysis and the alignment of the dark areas (Ag and Te) with lighter separation channels (related with atoms of low atomic number). It seems reasonable to propose that the formation of the 2D organometallic nanofibers could be originated from the spontaneous rearrangement directed by the coordination of Ag(I) towards Te atoms. The phenyl group seems to be allocated around the coordination chain …Ag-Te-Ag-Te…, which can contribute to stabilize the fibrillar-like nanostructure by π-π interactions between the rings.

Furthermore, the FTIR-ATR confirmed the presence of phenyl groups in the nanostructure (see **Figure S7**). The signals at 1570 cm^{-1}, 1470 cm^{-1}, 1432 cm^{-1} can be attributed to (C = C stretches), 1014 cm^{-1} to the C–H bending in-plane, C–H bending out-of-plane (726 cm^{-1}, 686 cm^{-1}) [8] and n(Te-C) (454 cm^{-1}).[11] Moreover, the spectra shows a very narrow peak at ca 1353 cm^{-1} that could be attributed to the ionic nitrate group in complex materials (**Figure S7**).[12]

Some tellurium containing materials derivatives are known to be semiconductor,[13] and it is well-documented how the electrical resistance of tellurium decreases with the addition of a few atoms of copper and antimony. To evaluate the conductivity of the AgTe nanowires, several studies were performed. The conductivity of AgTe nanowires was assessed through a quasi-DC transport method. The dried AgTe powder nanofibers were pressed into a pellet having a diameter of 3 mm and a thickness of

0.5 mm. This pellet was subsequently cut into bars having a width of approximately 1.5 mm. Electrical contacts to Pt wires were attached using Ag paint (Dupont 4929 N) in a four-terminal configuration. A current source meter (Keithley 6221) was used to inject a continuous current whose sign was periodically flipped, and the voltage was measured in Delta mode via a nanovoltmeter (Keithley 2182a). At room temperature, the pellet's resistance was strongly current-dependent, stabilizing at a value of ~ 7 GW cm when the current was reduced to 50 picoA. This resistivity value should be taken as a lower bound since further decreasing the current leads to strong fluctuations in the measured value, implying that it might be higher. Therefore, the TeAg organometallic nanofibers are strongly insulating at room temperature, probably due to the phenyl groups that cover the Ag-Te channels.

Being the nanofibers almost non-emissive materials, we discovered that the treatment with oleylamine (OA) under ultrasound resulted in highly red emissive fluorescent solution formation. As shown in Fig. 2A, the interaction of OA with the nanofibers resulted in a 24 nm redshift of the absorption peak at higher energies. Although a solvatochromic effect could be behind this observed offset, the peak at higher energy did not show this behaviour, remaining constant at 568 nm, although with a remarkable intensity. Interestingly, a strong red emission was observed, with a fluorescence band centred at ca. 606 nm when excited at 490 nm (Fig. 2B).

The emission intensity increases after OA treatment, suggesting that the nanofibers suffer an aggregation emission-induced process in which the long nanofibers connect between them. HRTEM and HAADF-STEM studies showed that the fluorescent nanofibers exhibited dark spots rather than channel alignment, like in the non-fluorescent starting material (Figs. 2C-D).

Confocal fluorescence microscopy imaging studies revealed that the fluorescence emission originated from the organometallic nanofiber rather than a discrete nanostructure isolated from the nanofibers (see Fig. 2F). Resembling the initial organometallic nanofibers, where the electron beam irradiation led to the degradation of the nanostructure, now, remarkably, certain regions of the nanofibers showed a rapid crystal growth upon exposure to the electron beam (see **Figure S9**).

Unfortunately, the rapid evolution of nanofibers limits the accurate analysis of the crystal structures observed in fluorescent nanofibers.

Table 1
Absorption in solution (λ_{abs}), emission maximum in solution (λ_{em}), Stokes shift (DI), emission maximum in the solid state (λ_{em}^{Solid}), and fluorescence lifetime (t) of the purified and oleyl amine stabilized fluorescent nanofibers in hexane.

λ_{abs} [nm]	λ_{em} [nm]	DI [nm]	λ_{em}^{Solid} [nm]	t[ns]
568	606	285714.29	610	T_1 = 3.23 T_2 = 5.65

To complete the study of the photophysical properties of the OA-activated nanofibers, the UV-vis absorption, emission, and excitation spectra in hexane solution and the emission in the solid state were obtained (Fig. 3). The matching found between the absorption and excitation spectra probes the purity of the samples (Fig. 3A). Moreover, the solution and solid spectra emission are almost coincident, suggesting a similar aggregation effect. The live time excited-state fluorescent spectra were obtained for the OA derivative being a biexponential with two times of 3.23 ns (residual) and a second component with 5.65 ns. (Table 1**and** Fig. 3D)

Temperature-dependent studies in the solid state were performed following the emission upon exciting at 490 nm, using a fibre optic device connected to the spectrofluorometer to explore the thermostability. Figure 3B-3C, shows the emission spectra which increase in intensity with the temperature ranging from 25ºC up to 80ºC, and later constantly decreasing from 90 to 130ºC. After this temperature ranges, the emission was totally quenched. Figure 3e-3F shows the cooling steep. The fibres were stable enough after cooling (120ºC to 25ºC), recovering *ca.* of 67% of the initial emission intensity, attributed to probably the rearrangement mode in the solid-state and partial degradation. The temperature-dependent decay analysis shows a notable fitting to minimum square values, suggesting using these nanofibers as a nanothermometer for the ranges of 25–90ºC and 90–120ºC.

Conclusions

In conclusion, this study explores the reactivity of diphenyl ditelluride (DPDT) with $AgNO_3$ in acetonitrile at room temperature under an inert atmosphere. The reaction led to the formation of long nanofibers with a 10–20 nm thickness and intricate nano structure. High-resolution transmission electron microscopy (HRTEM) analysis revealed an alignment of dark areas (Ag and Te) along the fibers. Electron diffraction (ED) showed a pattern of rings that indicate the formation of small crystalline nanoclusters with an atomic percentage of ca. 53% of Ag and ca. 47% of Te. The organometallic nanofibers strongly insulate at room temperature due to an organic insulating shell formed by the phenyl groups. We observed that the organometallic nanofibers acquire a strong red-fluorescence emission after treatment with oleylamine under an inert atmosphere. These red emissive nanofibers can be explored as nano thermometers between 25 to 120 ºC. The strong fluorescence observed due to an Aggregation induced emission mechanism in the present study adds to the growing research on the versatility of diorganyl ditellurides as precursors of metal telluride nanomaterials, with potential applications in various fields such as optical, electrical, and nanomaterial synthesis.

Methods Experimental Details

Manipulations, transfers, and reactions were conducted under a nitrogen atmosphere using standard Schlenk techniques. A nitrogen purge was used on these solvents before use, and transfers to reaction vessels were via stainless steel cannula under a positive pressure of N_2. Diphenyl ditelluride 98% (DPDT), silver nitrate 99% ($AgNO_3$), and Oleylamine (OA) were purchased from Sigma-Aldrich and used as received. Acetonitrile was obtained from Carlo-Erba.

Synthesis Of Silver-telluride Organometallic Nanofibers

$AgNO_3$ (34.5 mg, 0.5 mmol) was loaded into a Schlenk flask and dissolved with 45 mL of acetonitrile at RT. DPDT was dissolved in deoxygenated CH_3CN and syringed in the silver solution under magnetic stirring. After injection of DPDT the reaction acquired change from yellow to intense red colour in the first minute. After 30 minutes under stirring was observed the formation of a blood-red precipitate with fibrous aspect which was isolated using centrifugation (9000 rpm x 10 min) and finally resuspending in acetonitrile.

Synthesis Of Highly Fluorescent Silver-telluride Nanofibers

First, the organometallic nanofibers were synthesized as explained above. After 30 minutes, the solvent was removed via rota evaporation, obtaining a red solid. In the same vessel under inert atmosphere, 50 mL of previously deoxygenated oleylamine were introduced. The vessel was placed in an ultrasonic bath and kept under irradiation for 30 min. During this time the nanofiber solution turned a deep pink colour and more important with intense pink-fluorescence emission.

Physical Measurements

The extinction spectra were recorded using a JASCO 650 UV – Vis spectrophotometer provided by the PROTEOMASS Scientific Society-BIOSCOPE facility (Caparica, Portugal). All spectra were recorded using a HELMAQ10 1 cm light path quartz cell, while emission and excitation spectra have been carried out on a Horiba-Jobin-Yvon Fluoromax-4 spectrofluorometer in the PROTEOMASS Scientific Soceity-BIOSCOPE facilities. Emission spectra of the samples in the solid state were carried out on a Horiba Jovin-Yvon Fluoromax-4 spectrofluorometer coupled with a fiber-optics device connected to the spectrofluorometer by exciting the compound at an appropriate wavelength, in the PROTEOMASS-BIOSCOPE facilities. Temperature-dependent studies were performed by varying the temperature from 25 to 130°C using glass cells. Tempro Fluorescence Lifetime System with a Nanoled pulsed diode controller from Horiba Jobin-Yvon (Proteomass Scientific Society Facilities) was used to perform lifetime measurements.

Low magnification bright field transmission electron microscopy (BF-TEM) images were obtained using a JEOL JEM 1010 TEM microscope, working at 100 kV from the CACTI, University of Vigo (Spain). A JEOL JEM 2010F field-emission gun TEM working at 200 kV was used to obtain HRTEM images. To prepare samples, ten microliters of solution were dropping cast onto a Formvar-coated 400-mesh copper grid (Ted-pella, Inc.) and dried in air.

Current source Keithley 6221 (Keithley is the brand which was bought by Tektronix), Nanovoltmeter Keitheley 2182A (coupled to the current source for Delta mode). The sample was mounted on a Physical Parameter Measuring System (PPMS) sample puck (electrical transport puck P102), itself plugged on a PPMS Sample Wiring Test Station (model P150). Measurements were performed at room T, in air.

Delta mode: Continuous square pulses (width of ~ 20 ms) of electrical current having positive and negative values were sent to the sample. The respective voltage is measured by subtracting the positive voltage values from the negative ones, to subtract any parasitic voltage in the circuitry. 25 readings are averaged to yield the resistance value at any given second. The amplitude of the current was reduced by orders of magnitude to achieve nearly current independent readings. Very low currents lead to increased fluctuations in the readings, therefore ~ 7 GOhm cm should be taken as a lower bound with actual value being higher.

HAADF-STEM images were acquired using an aberration-corrected cubed FEI-Titan electron microscope operated at 120 kV and 300 kV.

Declarations

Acknowledgments

The authors acknowledge the financial support by the Associate Laboratory Research Unit for Green Chemistry-Clean Processes and Technologies-LAQV which is financed by national funds from FCT/MEC (UID/QUI/50006/2013) and co-financed by the ERDF under the PT2020 Partnership Agreement (POCI-01-0145-FEDER-007265), as well as the PROTEOMASS Scientific Society, General Funds 2021-2022 (Portugal) for funding support.

J.F.-L., A.F.-L.; C.L.; J.D.; and J.L.C.-M. thank the FCT-MEC for the research grant SiSi4Bacter (PTDC/QUI-COL/1517/2020). J.F.-L. thanks the FCT-UNL for the DL57/2016 Assistant Researcher Contract. F.D. thanks to FCT-MEC (Portugal) for his doctoral grant 2021.05161.BD. H.M S acknowledges the Associate Laboratory for Green Chemistry-LAQV (LA/P/0008/2020) funded by FCT/MCTES for his research contract. A.F.-L. thanks the research contract DL57 associated to the grant SiSi4Bacter (PTDC/QUI-COL/1517/2020).

A. A. Dos Santos thank FAPESP (2014/17310-5, 2016/09579-0 and 2018/24434-3), IQ-USP and CNPq (401797/2013-9) for financial support. L.B. is supported by the US Department of Energy, Basic Energy Sciences program, through award DE-SC0002613. A portion of this work was performed at the National High Magnetic Field Laboratory, which is supported by the National Science Foundation Cooperative Agreement No. DMR-2128556 and the State of Florida. The authors acknowledge financial support from the European Commission under the Horizon 2020 programed by grant no. 731019 (EUSMI).

Author´s Contributions

J.D., J.F-L, and A.F-L performed the experiments, data analysis of fibber-synthesis section. B. R. G. perform TEM analysis. E.B. and S. B. study the nanofibers by HAADF-STEM. F.D and J.F-L performed the experiments related to photophysical studies. H.M.S perform the ESI MS spectrometry studies. A.F. S and L. B. performed the conductivity measurements. F.D. perform the photophysical studies in solution and solid state. J. F. L., C. L., A. d S. conceptualization. J.F-L and C.L. wrote the first manuscript draft. J. F-L,

A.F.L, C.L, J.L.C, A.d.S., and H.M.S obtained the funding for the project. All authors contributed to writing and correction of final draft, given approval for the final version of the manuscript.

Competing interests

All authors declare no competing interests.

References

1. Brutchey, R. L. Diorganyl Dichalcogenides as Useful Synthons for Colloidal Semiconductor Nanocrystals, *Acc. Chem. Res.*, **48**, 2918–2926 (2015).
2. Kisker, D. W., Steigerwald, M. L., Kometani, T. Y., & Jeffers, K. S. Low temperature organometallic vapor phase epitaxial growth of CdTe using a new organotellurium source *Appl. Phys. Lett.*, **50**, 1681–1683 (1987).
3. Schlecht, S., Budde M. & Kienle L. Nanocrystalline Tin as a Preparative Tool: Synthesis of Unprotected Nanoparticles of SnTe and SnSe and a New Route to $(PhSe)_4Sn$, *Inorg. Chem.*, **41**, 6001–6005 (2002).
4. Webber, D. H. & Brutchey R. L. Photolytic preparation of tellurium nanorods, *Chem. Commun.*, **2**, 5701–5703 (2009).
5. Sun, F., Hong, W., He, X., Jian, C., Ju, Q., Cai Q. & Liu, W. Synthesis of Ultrathin Topological Insulator *β*-Ag_2Te and Ag_2Te/WSe_2-Based High-Performance Photodetector, *Small*, **19**, 1–12 (2023).
6. Gautam, A. K., Singh H. H. & Khare N. Multifunctional flexible Ag_2Te-nylon nanocomposite freestanding film for harvesting thermal and mechanical energy, *Nano Energy*, **107**, 108125 (2023).
7. Fernandez-Lodeiro, J., Rodríguez-Gonzalez, B., Santos, H. M., Bertolo, E., Capelo, J. L., Dos Santos A. A. & Lodeiro, C. Unraveling the Organotellurium Chemistry Applied to the Synthesis of Gold Nanomaterials, *ACS Omega*, **1**, 1314–1325 (2016).
8. Fernández-Lodeiro, J., Rodríguez-Gónzalez, B., Novio, F., Fernández-Lodeiro, A., Ruiz-Molina, D., Capelo, J. L., Santos A. A. D. & Lodeiro C. Synthesis and Characterization of $PtTe_2$ Multi-Crystallite Nanoparticles using Organotellurium Nanocomposites, *Sci. Rep.*, **7**, 1–10 (2017).
9. Liaw W. & Pengs S. Synthesis and Characterization of Polymeric Ag(I)-Telluroether and Cu(I)-Diorganyl Ditelluride Complexes: Crystal Structures of $[Ag(MeTe(CH_2)_3TeMe)_2]_n[BF_4]_n$, $[(m_2\text{-}MeTeTeMe)Cu(m\text{-}Cl)]_n$, and $[Ag_2(NCCH_3)_4(m_2\text{-}(p\text{-}C_6H_4F)TeTe(p\text{-}C_6H_4F))_2][BF_4]_2$ *Inorg. Chem.*, **2**, 3755–3759 (1995).
10. Cuerva, C., Fernández-Lodeiro, J., Cano, M., Capelo-Martínez J. L. & Lodeiro C. Water-soluble hollow nanocrystals from self-assembly of AIEE-active Pt(II) metallomesogens, *Nano Res.*, **14**, 245–254 (2021).
11. Dos Santos, S. S., Cabral, B. N., Abram, U. & Lang, E. S. Bis(4-pyridyl)ditelluride as starting material for the synthesis of zwitterionic compounds and metal complexes, *J. Organomet. Chem.*, **723**, 115–121 (2013).

12. Lodeiro, C., Bastida, R., De Blas, A., Fenton, D. E., Macías, A., Rodríguez A. & Rodríguez-Blas T. Complexes of lead(II) and lanthanide(III) ions with two novel 26-membered-imine and -amine macrocycles derived from 2,6-bis(2-formylphenoxymethyl) pyridine, *Inorganica Chim. Acta*, **267**, 55–62 (1998).
13. Cartwright, C. H. & Haberfeld M. Conductivity of Tellurium,*Nature,* 1934, **134**, 287–288.

Figures

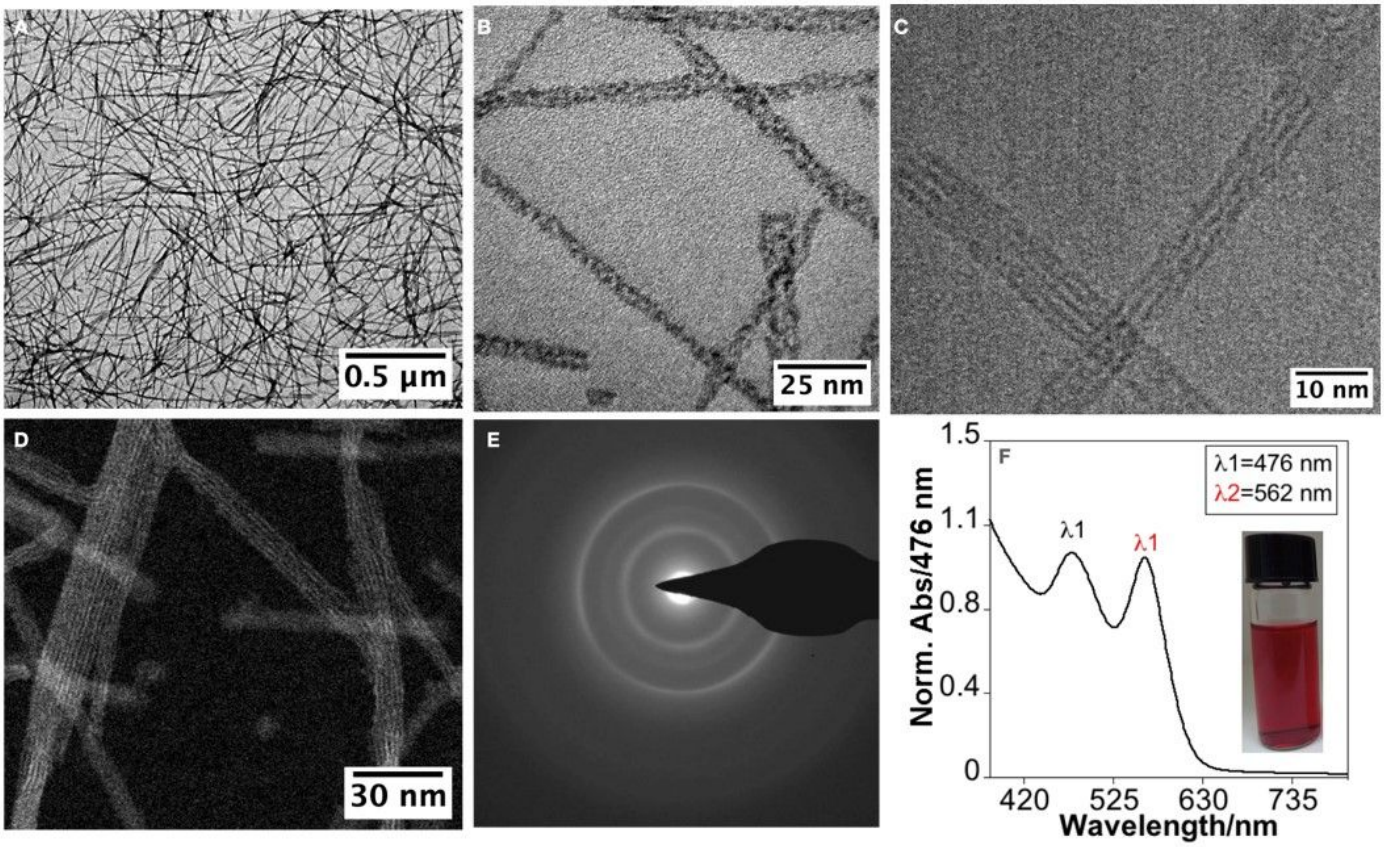

Figure 1

HRTEM images (A, B), bright-field STEM (C), HAADF-STEM (D) and electron diffraction pattern (E) of the nanofibers. Absorption spectra (F) of purified nanofibers in acetonitrile (inset in panel F shown the colour colloidal suspension of Nanofibers).

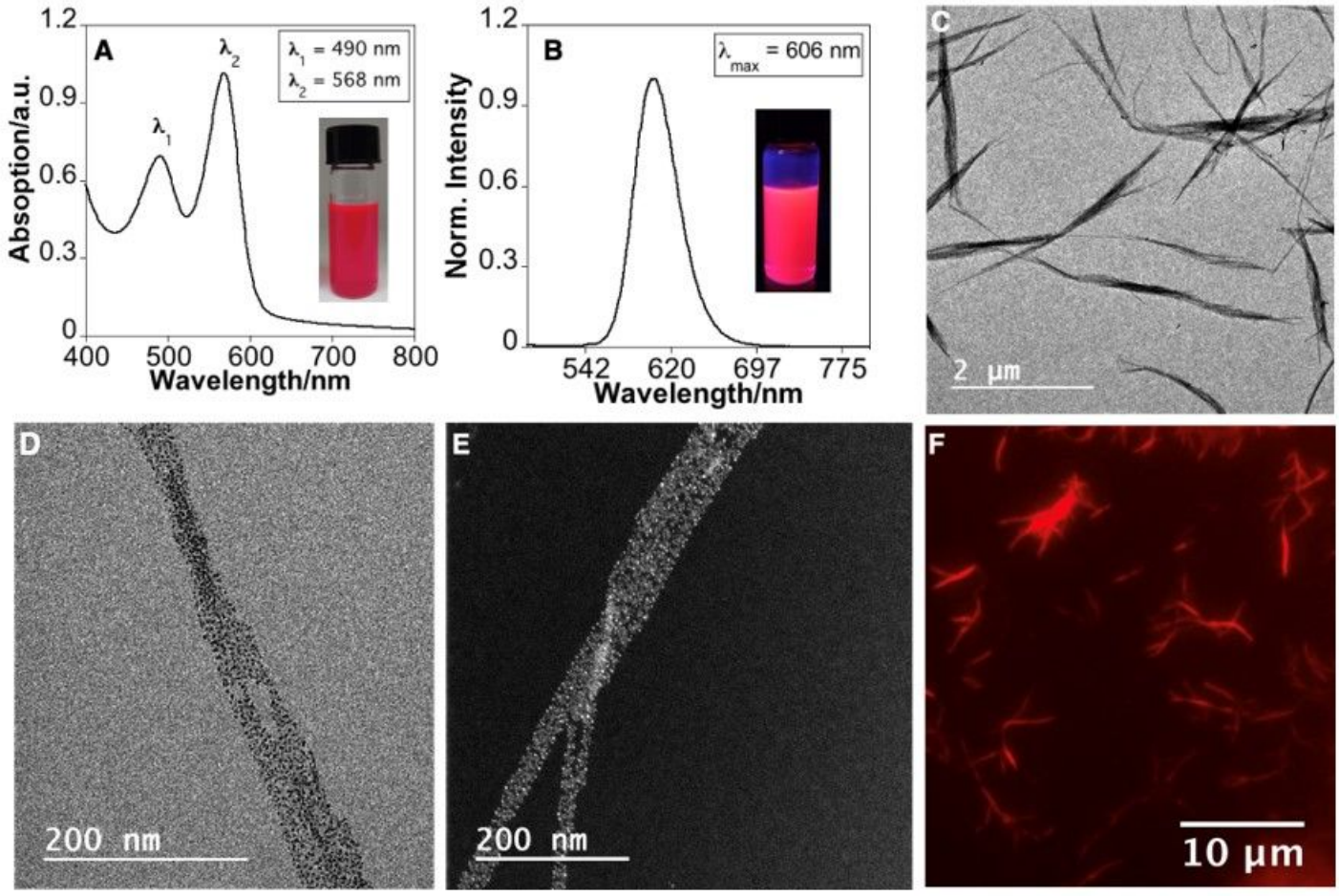

Figure 2

Absorption spectra (A) and fluorescence emission spectra (B) of purified and stabilized fluorescence nanofibers in hexane, after treatment with OA. l_{exc} = 490 nm (inset in panel A and B shown the colour solution of Nanofibers under normal and UV light respectively, l_{exc} = 490 nm). TEM (C, D), HAADF-STEM (E) and confocal fluorescence images (F) of the TeAg nanofibers.

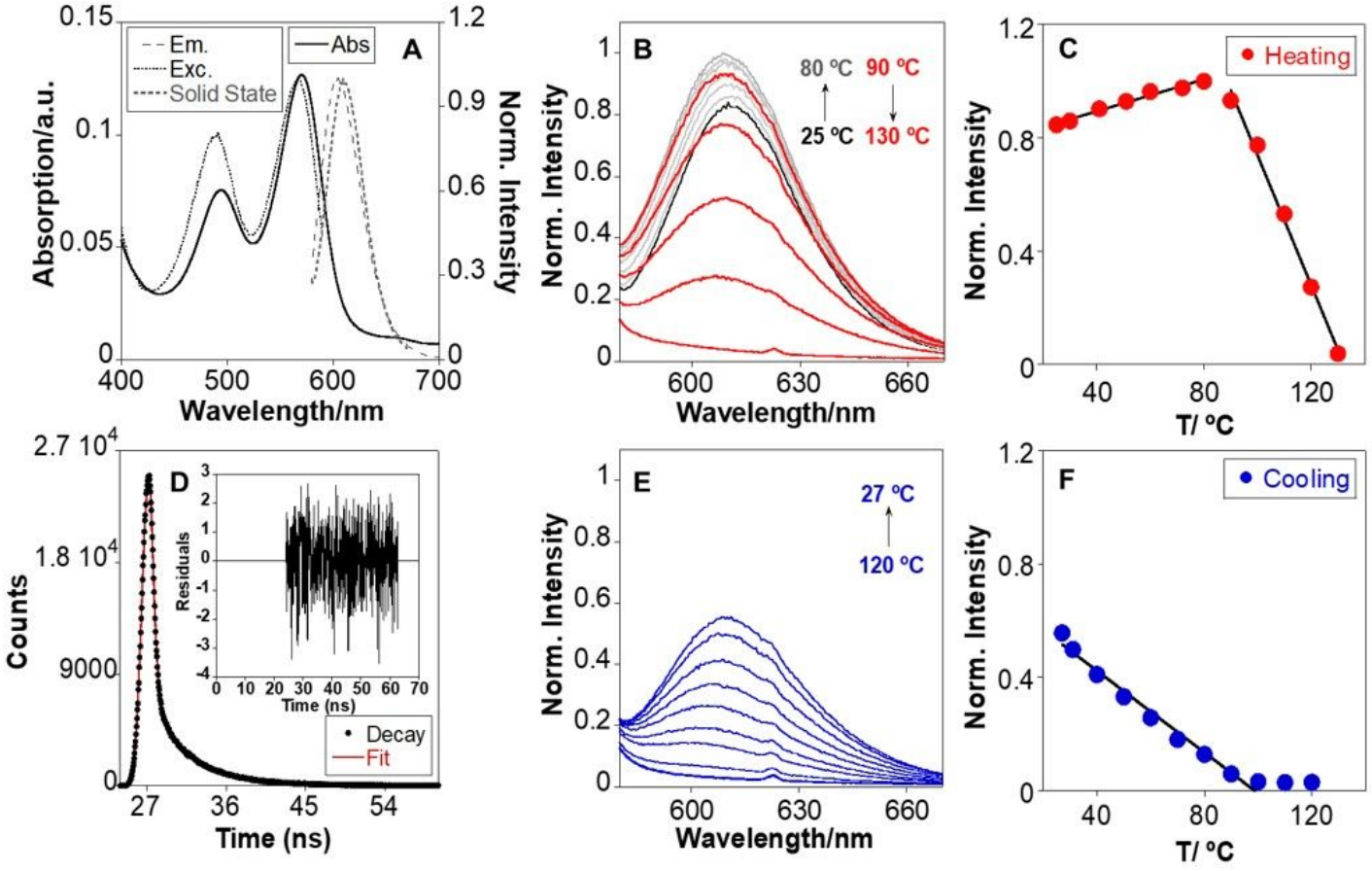

Figure 3

UV-vis Absorption, Emission and Excitation spectra in solution as well as the emission spectra in solid state (A). Temperature-dependent emission spectra (B) collected through a warming cycle between 25ºC to 130ºC. $I_{norm.}$ vs. T plot recorded in the emission maximum at 610 nm upon heating [25 to 80 ºC (Y= 0.78063 + 0.002818x, yielding R=0.99067; 90 to 130 ºC Y= 3.0273 – 0.022888x yielding R=0.99687] (C). Life-time decay and fitting of the purified and oleyl amine stabilized fluorescent nanofibers in hexane, l_{exc}=570 nm (D). Temperature-dependent emission spectra (E) in a cooling cycle between 120ºC to 27ºC. $I_{norm.}$ vs. T plot recorded in the emission maximum at 610 nm upon cooling [100 to 27 ºC (Y= 0.71185 – 0.0072105x, yielding R=0.99103)].

Supplementary Files

This is a list of supplementary files associated with this preprint. Click to download.

- TableofContents.docx
- SIJLodeiroetalCC2023.docx